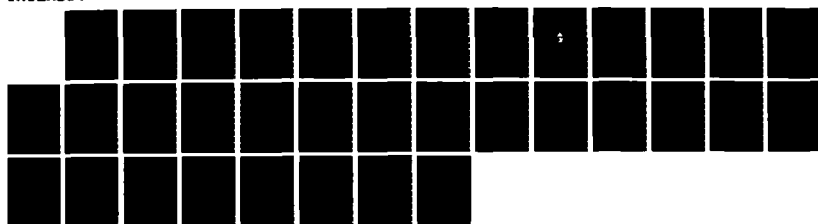
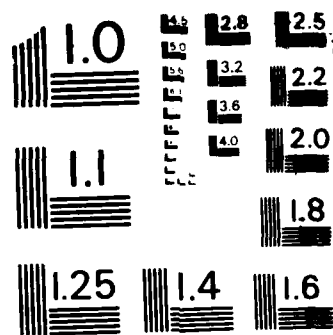


NO-A176 815

POTENTIAL MODULATIONS ON SCATHA (SPACECRAFT CHARGING AT 1/1  
HIGH ALTITUDE) SP. (U) AEROSPACE CORP EL SEGUNDO CA  
SPACE SCIENCES LAB P D CRAVEN ET AL. 30 SEP 86  
UNCLASSIFIED TR-0006(6940-05)-13 SD-TR-86-92 F/G 4/1 ML





MICROCOPY RESOLUTION TEST CHART  
NATIONAL BUREAU OF STANDARDS-1963-A

12

AD-A176 815

## Potential Modulations on the SCATHA Spacecraft

P. D. CRAVEN and R. C. OLSEN  
Marshall Space Flight Center  
Huntsville, AL 35812

T. AGGSON  
Goddard Space Flight Center  
Greenbelt, MD 20771

and

J. F. FENNELL and D. R. CROLEY, JR.  
Space Sciences Laboratory  
Laboratory Operations  
The Aerospace Corporation  
El Segundo, CA 90245

30 September 1986

Prepared for  
SPACE DIVISION  
AIR FORCE SYSTEMS COMMAND  
Los Angeles Air Force Station  
P.O. Box 92960, Worldway Postal Center  
Los Angeles, CA 90009-2960

APPROVED FOR PUBLIC RELEASE.  
DISTRIBUTION UNLIMITED

STAMP  
FEB 19 1987  
E

FILE COPY

87 2 19 064

This report was submitted by The Aerospace Corporation, El Segundo, CA 90245, under Contract No. F04701-85-C-0086 with the Space Division, P.O. Box 92960, Worldway Postal Center, Los Angeles, CA 90009-2960. It was reviewed and approved for The Aerospace Corporation by H. R. Rugge, Director, Space Sciences Laboratory.

Capt Douglas R. Case/YCM was the project officer for the Mission-Oriented Investigation and Experimentation (MOIE) Program.

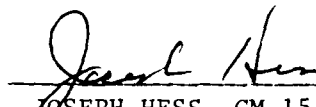
This report has been reviewed by the Public Affairs Office (PAO) and is releasable to the National Technical Information Service (NTIS). At NTIS, it will be available to the general public, including foreign nationals.

This technical report has been reviewed and is approved for publication. Publication of this report does not constitute Air Force approval of the report's findings or conclusions. It is published only for the exchange and stimulation of ideas.



---

DOUGLAS R. CASE, Capt, USAF  
MOIE Project Officer  
SD/YCM



---

JOSEPH HESS, GM-15  
Director, AFSTC West Coast Office  
AFSTC/WCO OL-AB

UNCLASSIFIED

SECURITY CLASSIFICATION OF THIS PAGE (When Data Entered)

REPORT DOCUMENTATION PAGE		READ INSTRUCTIONS BEFORE COMPLETING FORM	
1. REPORT NUMBER SD-TR-86-92	2. GOVT ACCESSION NO. <b>AD-A176 813</b>	3. RECIPIENT'S CATALOG NUMBER	
4. TITLE (and Subtitle) POTENTIAL MODULATIONS ON THE SCATHA SPACECRAFT		5. TYPE OF REPORT & PERIOD COVERED	
7. AUTHOR(s) P. D. Craven, R. C. Olsen, T. Aggson, J. F. Fennell, and D. R. Croley, Jr.		6. PERFORMING ORG. REPORT NUMBER TR-0086(6940-05)-13	
9. PERFORMING ORGANIZATION NAME AND ADDRESS The Aerospace Corporation El Segundo, CA 90245		8. CONTRACT OR GRANT NUMBER(s) F04701-85-C-0086	
11. CONTROLLING OFFICE NAME AND ADDRESS Space Division Los Angeles Air Force Station Los Angeles, CA 90009-2960		10. PROGRAM ELEMENT, PROJECT, TASK AREA & WORK UNIT NUMBERS	
14. MONITORING AGENCY NAME & ADDRESS (if different from Controlling Office)		12. REPORT DATE 30 September 1986	
		13. NUMBER OF PAGES 30	
		15. SECURITY CLASS. (of this report) Unclassified	
		15a. DECLASSIFICATION/DOWNGRADING SCHEDULE	
16. DISTRIBUTION STATEMENT (of this Report) Approved for public release; distribution unlimited.			
17. DISTRIBUTION STATEMENT (of the abstract entered in Block 20, if different from Report)			
18. SUPPLEMENTARY NOTES			
19. KEY WORDS (Continue on reverse side if necessary and identify by block number) Charging Thermal Plasma Satellite Potential			
20. ABSTRACT (Continue on reverse side if necessary and identify by block number) A small (1 volt) modulation of the spacecraft potential is observed on the SCATHA satellite through its effects on four instruments, two particle detectors and two field detectors. We show that there is a strong causal link between the modulation of the potential at this 1 volt level and a non-uniform distribution of the photo-emissive properties of the conducting material on the surface of the satellite.			

DD FORM 1473  
(FACSIMILE)

UNCLASSIFIED

SECURITY CLASSIFICATION OF THIS PAGE (When Data Entered)

## CONTENTS

I.	INTRODUCTION.....	5
A.	Satellite Charging.....	5
B.	SCATHA.....	6
C.	Instrument Description.....	6
II.	OBSERVATIONS.....	11
A.	LIMS.....	11
B.	UCSD Sheath Effects Instrument.....	14
C.	GSFC Electric Field Monitor.....	16
D.	Eclipse.....	18
E.	Photosheath.....	20
F.	Summary of Observations.....	21
III.	ANALYSIS.....	23
IV.	CONCLUSIONS.....	29
	REFERENCES.....	31

Accession For	
NHS GR&I	<input checked="" type="checkbox"/>
DIC TAG	<input type="checkbox"/>
Unpublished	<input type="checkbox"/>
Journal Title _____	
Page _____	_____
Date _____	_____
Author _____	_____
Title _____	_____
Topic _____	_____
A-1	



## FIGURES

1.	Plan View of All the Instruments on the SCATHA Satellite.....	7
2.	Effect of the Satellite Potential Change on the LIMS Data.....	12
3.	Plot of H <sup>+</sup> Counts per Accumulation Period for the LIMS.....	13
4.	Typical Potential Response of the Short Booms of the Sheath Effect Monitor.....	15
5a.	Eclipse Behavior of the Field Detectors; the Behavior of the GSFC Electric Field Monitor.....	17
5b.	Eclipse Behavior of the Field Detectors; the Behavior of the Short Booms of the Aerospace Sheath Monitor.....	19
6.	Modulation Cycle of All the Instruments Plotted in the Spin Phase Angle of the LIMS.....	22
7.	Distribution of Grounded Conducting Exterior Surfaces on SCATHA.....	24
8.	Plot of the Photoemissive Yield Model of SCATHA Used to Calculate the Total Photocurrent.....	25
9.	Total Photocurrent of Illuminated Grounded Exterior Conducting Surfaces as a Function of the +Z-Sun Angle.....	27

## I. INTRODUCTION

### A. SATELLITE CHARGING

Proper analysis of thermal plasma and electric field data from satellites requires an accurate knowledge of the satellite potential. The magnitude of the potential is determined in equilibrium by the requirement that the currents to and from the satellite sum to zero. This includes not only the ambient electron and ion current to the satellite but also material dependent currents from the satellite such as from photoelectrons and secondary electrons. Thus both the plasma environment and the properties of the material on the surface of the satellite play a role in the charging process. Passive control of the potential has been attempted by careful design and selection of the material used on the satellite and in particular by making the exterior surfaces conductors. This method appears to have been successful on the GEOS 2 satellite (Knott, 1984) in that it did not charge to large potentials. The potential of GEOS 2 typically floated between 4 and 10 volts positive (Knott, 1984). For particle detectors, a nonzero potential prevents the measurement of the full energy spectrum of the population. This has been a particularly bothersome problem for low energy ion measurements. For example, there is evidence from geosynchronous satellites that positive potentials cause some low energy populations to be hidden (Olsen, 1982). Such populations can be observed if the detector potential is actively controlled (Sojka et al., 1984).

For spinning spacecraft, changes in the potential that are phased with the spin period are also a problem in that the flux or count measurements can be highly modulated (DeForest and McIlwain, 1971; DeForest, 1973; Sojka et al., 1984). A spin modulation of the potential distorts the measurements not only of particle detectors but also of field detectors as will be seen later. It is therefore important to be aware of the existence of a potential modulation. It is also important to know the cause of such modulations so that steps can be taken on future spacecraft to avoid them.



It is the purpose of this report to discuss a small amplitude (f1 volt), spin phased modulation of the potential of the conducting surfaces on the SCATHA satellite and to suggest a possible cause. We will first show the effects of the potential modulation on four instruments, two particle detectors and two field detectors, which are distributed over the satellite. These effects and the positions of the instruments will then be used to show that the modulation appears to be caused by a combination of a nonuniform distribution of the area of surface conducting material that is grounded to the satellite frame and differing photoemissive properties for the conducting material.

#### B. SCATHA

The Air Force P78-2 satellite, also known as SCATHA (Spacecraft Charging at High Altitude), was designed to study the causes and dynamics of spacecraft charging, specifically at geosynchronous orbit. The satellite is basically a cylinder, approximately 1.75 m in both length and diameter. It is spin stabilized at about 1 rpm with its spin axis in the orbit plane and perpendicular to the earth-sun line. Many of the instruments are contained in an area around the middle of the cylinder (see Figure 1), the so-called belly band. Both insulating and conducting material are contained in the belly band. Solar cells cover most of the remaining sides of the cylinder. SCATHA is in a nearly geosynchronous orbit with a period of 23.5 hours, an apogee of 7.3 Re and a perigee of 5.8 Re. A description of the program and the satellite has been given by Fennell (1982) and Stevens and Vampola (1978).

#### C. INSTRUMENT DESCRIPTION

The four instruments used in this study are the NASA/Goddard Space Flight Center electric field monitor (SC10), The Aerospace Corporation sheath field monitor (SC2), the NASA/Marshall Space Flight Center light ion mass spectrometer (SC7), and the University of California at San Diego charged particle experiment (SC9). The location of each of these instruments is shown in Figure 1. The designations SC2, SC9, etc., are shorthand notations for each of the instruments on SCATHA. They have no special significance other than for accounting purposes.

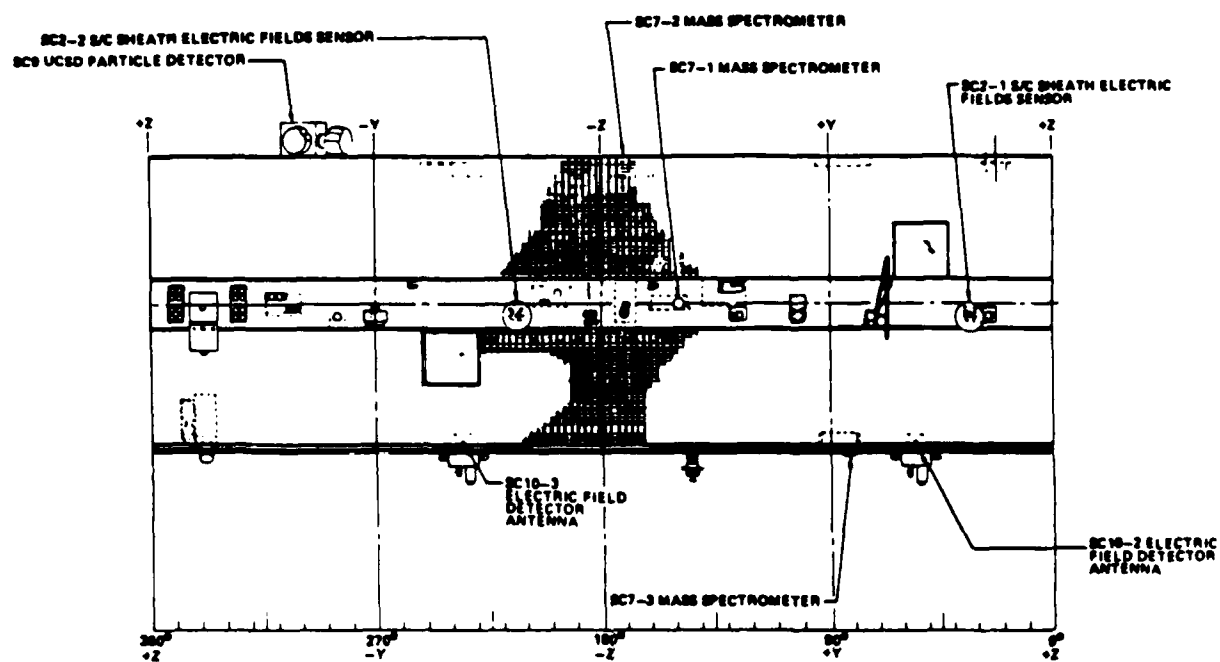


Figure 1. Plan View of All the Instruments on the SCATHA Satellite

The Aerospace sheath electric field monitor measures the floating potential of two Aquadag coated spheres relative to the spacecraft ground. The spheres have a diameter of about 18 cm and are mounted 3 m from the satellite surface on booms that are 180 deg apart and that are near the centerline of the satellite. Each sphere has a 25.4 cm long shadow stub on the side of the spherical probe away from the spacecraft (see Figure 7) that balances the shadowing effect of the 3 m support booms when the potential difference between the two probes is being measured. This instrument also contains particle detectors, but the data from them are not used here.

The NASA/GSFC electric field detector is a cylindrical double floating ensemble for measuring electric fields. Dipole antennas which are 100 m tip to tip in length are used as the floating probes. The antenna wire is composed of beryllium copper. Each of the antennas is insulated except for the last 20 m, which is the active part. Differential signals between the antennas give the ambient electric field. Common mode measurements also made with this instrument give the potential of one probe relative to spacecraft ground. The data which are used below are taken from the common mode measurements. The antennas were slowly deployed starting in late February and ending in early March 1979.

The NASA/MSFC light ion mass spectrometer (LIMS) is described in detail by Reasoner et al. (1982). A retarding potential analyzer was used in conjunction with a magnetic mass spectrometer to measure the total flux and energy distribution (for energies less than 100 eV) of  $H^+$ ,  $HE^+$ , and  $O^+$ . There are three sensors associated with this instrument. One views radially from the belly band, one parallel to the spin axis from the forward end of the satellite, and one antiparallel to the spin axis from the aft end. The radial sensor samples a wide range of pitch angles as the satellite spins, while the other two sample pitch angles near 90 deg. All of the sensors operate together, i.e., all are set for the same ion at the same time, and all have the same retarding potential at the same time. The output of the radial sensor is sampled twice as often as that of the other two sensors. Each of these sensors is mounted flush with the satellite surface as shown in Figure 1. An electronics failure in the LIMS on February 17, 1979 prior to the

deployment of the electric field booms prevented the acquisition of data simultaneously with the electric field detector.

The UCSD charged particle experiment is an electrostatic analyzer that measures both ion and electron flux. This instrument, except for the energy range of the detectors, is identical to the UCSD Auroral Particles Experiment on AT-6 (Mauk and McIlwain, 1975). All three of the sensors of this instrument are contained in a single package that is mounted at the forward end of the satellite as shown in Figure 1. Data shown in this article are from the sensor that has a radial viewing direction that is fixed relative to the satellite body. The energy range of this sensor is 1 eV to 2 keV with an energy resolution ( $\Delta E/E$ ) of 20%. The angular field of view is  $5 \times 7$  deg. The output of the fixed detector is sampled 8 times/second in the modes used for this work. In order to measure the angular distributions of a given energy ion, the detector dwelled at a fixed energy range for 64 seconds. The differential measurement characteristics of this instrument complement the integral nature of the measurements of the LIMS.

## II. OBSERVATIONS

### A. LIMS

The satellite potential modulation dramatically affects the thermal plasma measurements. This is shown in Figure 2, which exhibits the count rates from all three LIMS sensors as a function of time. All three sensors show a minimum in counts when the sun angle of the radial sensor is about 180 deg. The LIMS radial sensor (sensor 1) shows a minimum in counts twice per spin period because there is also an anisotropy in the plasma angular distribution that is not related to the potential modulation. The fact that all three sensors do not have two minimums per spin period suggests that the simultaneous minimum in counts that is recorded is caused by a change in the spacecraft potential rather than environmental variations. Comparisons of this LIMS data with that of the sheath effects monitor during the initial operations of SCATHA showed that both instruments exhibited evidence of a potential change at the same time (D. L. Reasoner, private communication). Subsequent analysis has shown that the potential modulation effect is also evident in the data from the electric field monitor and the charged particle instrument. The phasing of the modulation in the satellite spin is the same with respect to the sun angle for all the instruments, as will be shown below. The effect is first shown for each of the instruments individually and then as a group.

Figure 3 shows an expanded view of the H<sup>+</sup> count rate at zero retarding potential for the LIMS radial detector (Sensor 1) and one of the end detectors (Sensor 2), both plotted as a function of the spin angle of sensor 1. The spin angle is measured from the equatorial plane and is zero when the LIMS radial sensor's look direction is in the equatorial plane and in the sunward direction. The position of the sun in terms of the spin angle will vary according to the time of the year. For the data in Figure 3, the angle between the look direction of the radial detector and the satellite-sun line is a minimum at a spin angle of about -15 deg. The S at the bottom of the figure marks this position. The RAM angle, the angle between the look

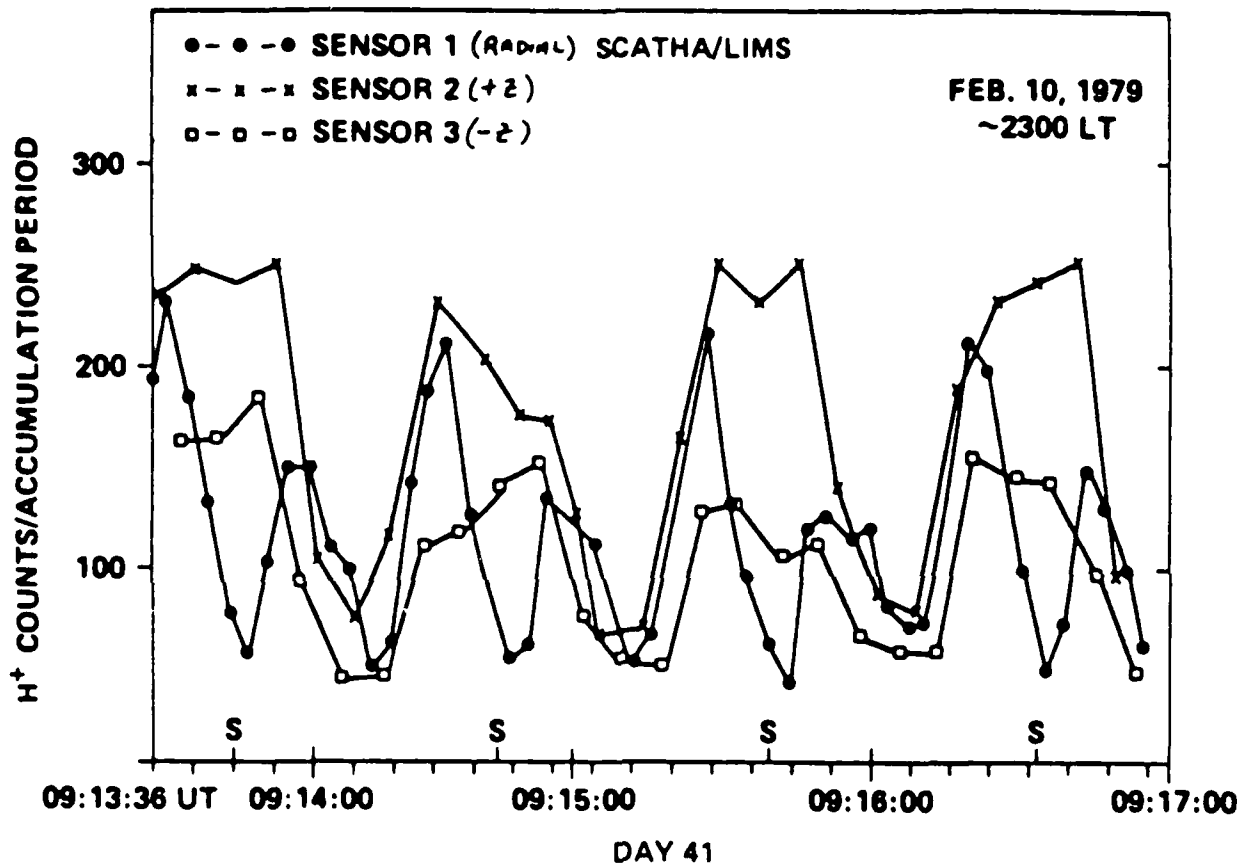


Figure 2. Effect of the Satellite Potential Change on the LIMS Data. The radial head was looking sunward at the positions marked with an S.

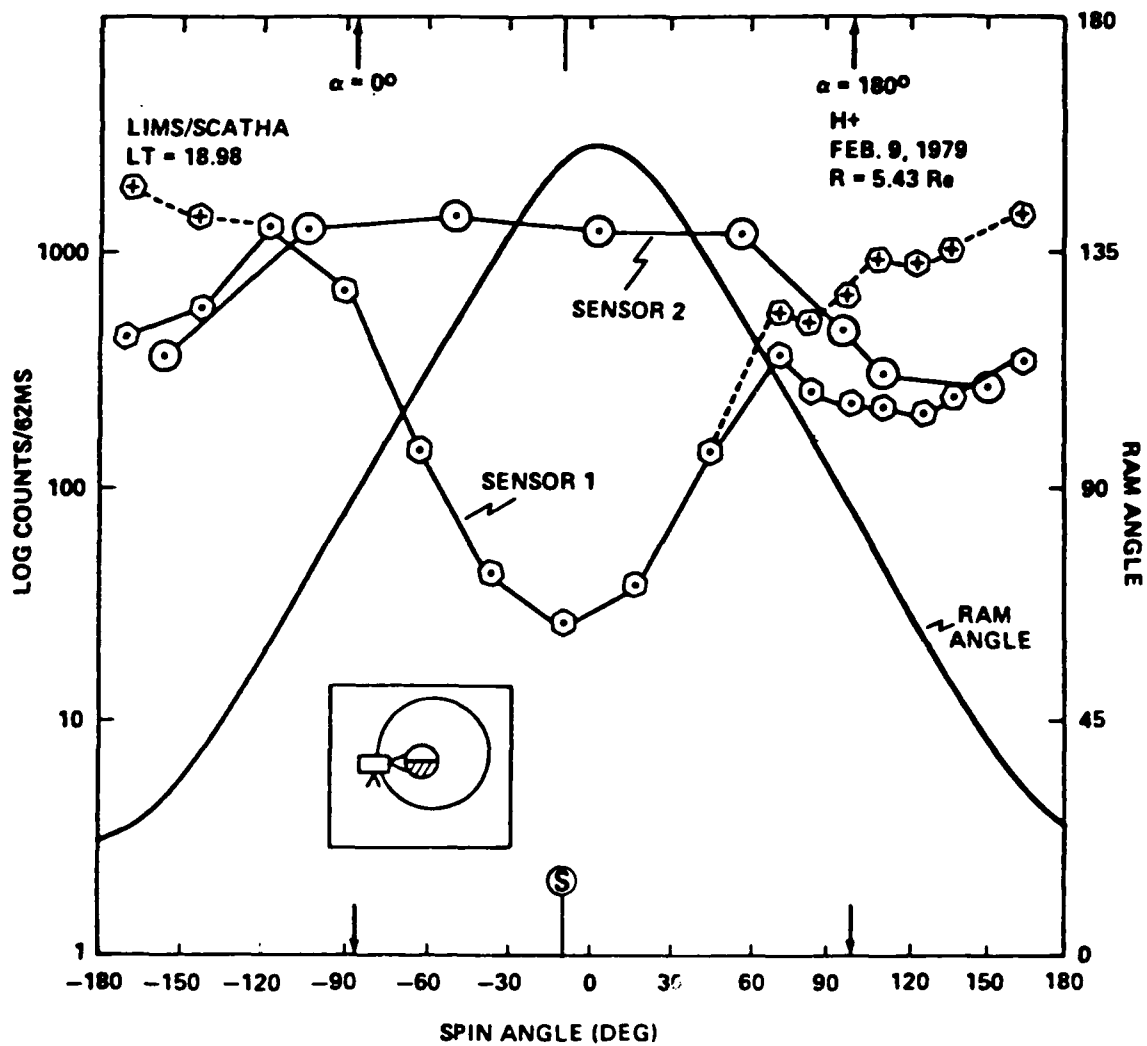


Figure 3. Plot of H+ Counts per Accumulation Period for the LIMS. The sun is at the position marked S at this time of the year. The RAM angle plot applies only to the radial head.

direction of the radial sensor and the spacecraft velocity, is plotted in Figure 3 as the solid line and applies only to the radial sensor. The scale for the RAM is plotted on the right vertical axis. Although the end detector does not change look directions during a spin, the data are plotted against spin angle in order to show the spin induced variation in ion count rate. As shown in Figure 3, which is a typical spin plot for the time frame indicated, there is a plateau in the count rate of sensor 2 from about -110 to 60 deg. The count rate falls to lower values at other spin angles. Since the end sensors do not vary in RAM or pitch angles over a spin period, the decrease in the count rate for sensor 2 indicates that the spacecraft potential is changing, becoming more positive.

The uncorrected data from sensor 1 (the solid line) show an angular distribution that might be identified as a pitch angle variation in the absence of other information. The minimum and maximum pitch angles are shown by the arrows in Figure 3. Since the three sensors operate together and are measuring total ion flux, one can correct, at least to first order, for the potential modulation of the flux into the radial detector by using the data from sensor 2. The ratio of the counts from this sensor in the portion of the curve where the potential is least positive (the plateau) to the counts at a given spin angle is a factor that can be applied to the data from the radial sensor to remove the effects of the potential change during a spin period. Such a correction using the sensor 2 data when applied to the sensor 1 data yields the dotted curve in Figure 3. The corrected curve shows that the plasma peaks in the RAM direction, i.e., where the RAM direction is smallest. This indicates an isotropic cold plasma. Energy analysis from the LIMS confirms that the plasma has a cold ( $kT < 1\text{eV}$ ) component at this time. The difference between the corrected and the uncorrected data in this figure indicates the importance of removing the effects of charging from the data before inferring the basic plasma characteristics.

#### B. UCSD SHEATH EFFECTS INSTRUMENT

The sheath effects instrument also shows the effect of a change in potential during a spin. Figure 4 shows a typical response of the boom



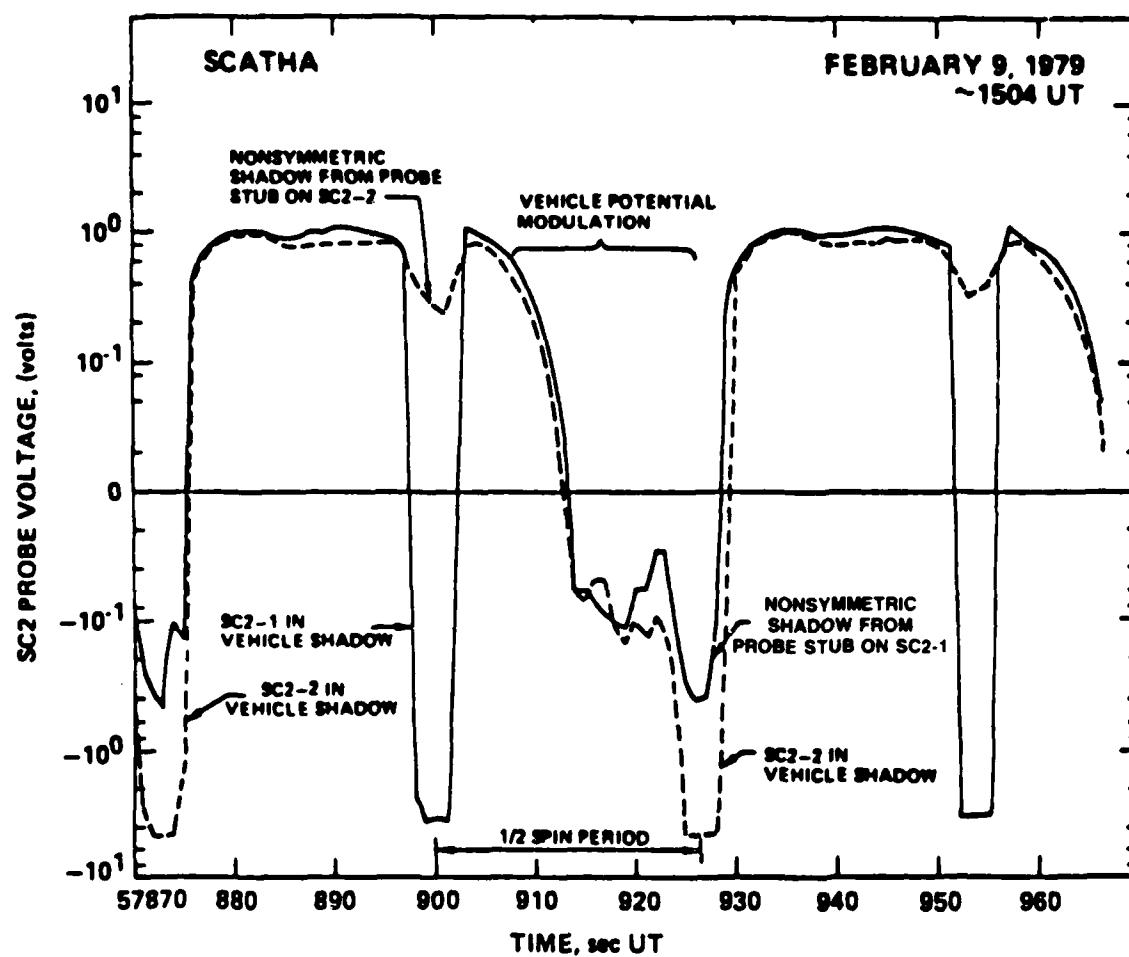


Figure 4. Typical Potential Response of the Short Booms of the Sheath Effect Monitor

mounted spheres. The sphere voltage measured relative to the spacecraft is plotted as a function of time. For each of the spherical probes, a variation in the sun illumination will change the amount of photoemission which will alter the charge of the probe and therefore its potential relative to the spacecraft. Shadowing of the spheres reduces the illuminated area of the spheres and thus the number of electrons emitted through photoemission, causing the spheres to drop in potential. This effect is seen in the response of the probes as the dip in probe voltage due to the nonsymmetric shadow of the probe stub (at 57,900 seconds UT in Figure 4 for SC2-2 and 57,925 seconds UT for SC2-1) and also as the large decrease due to shadowing of the probes by the spacecraft. A variation in the spacecraft ground potential will result in an apparent variation in the probe common mode voltage. In an isotropic plasma, the character of which is not changing with time, the potential of the spheres with respect to the satellite should follow a symmetric curve in a potential versus sun angle plot. The symmetry of the curve will be lost if the spacecraft ground potential changes during the spin period. The effect is seen in Figure 4 for both probes from about 57,905 to 57,925 seconds UT. Except for the time in the spacecraft shadow and the nonsymmetric shadow from the probe stub, the illuminated area of the spheres does not change during this part of the spin; therefore, the decrease in the probe voltage indicates that the spacecraft ground has increased (gone positive relative to the probes). The magnitude of the change is about 1 volt. The long electric field antenna had not been deployed at this time but shows similar behavior once deployed.

#### C. GSFC ELECTRIC FIELD MONITOR

The common mode voltage for one of the electric field antennas (SC10-2) is shown in Figure 5a. Time is plotted along the horizontal axis. The common mode voltage for this instrument is also measured relative to spacecraft ground. The response of the antenna is similar to the sheath potential probe in that changes in probe illumination cause changes in photoemission which in turn cause the potential of the antenna relative to spacecraft ground to vary (Lai and Cohen, 1984). The antenna are cylindrical so that the illumination changes drastically with sun angle, having two positions with grazing

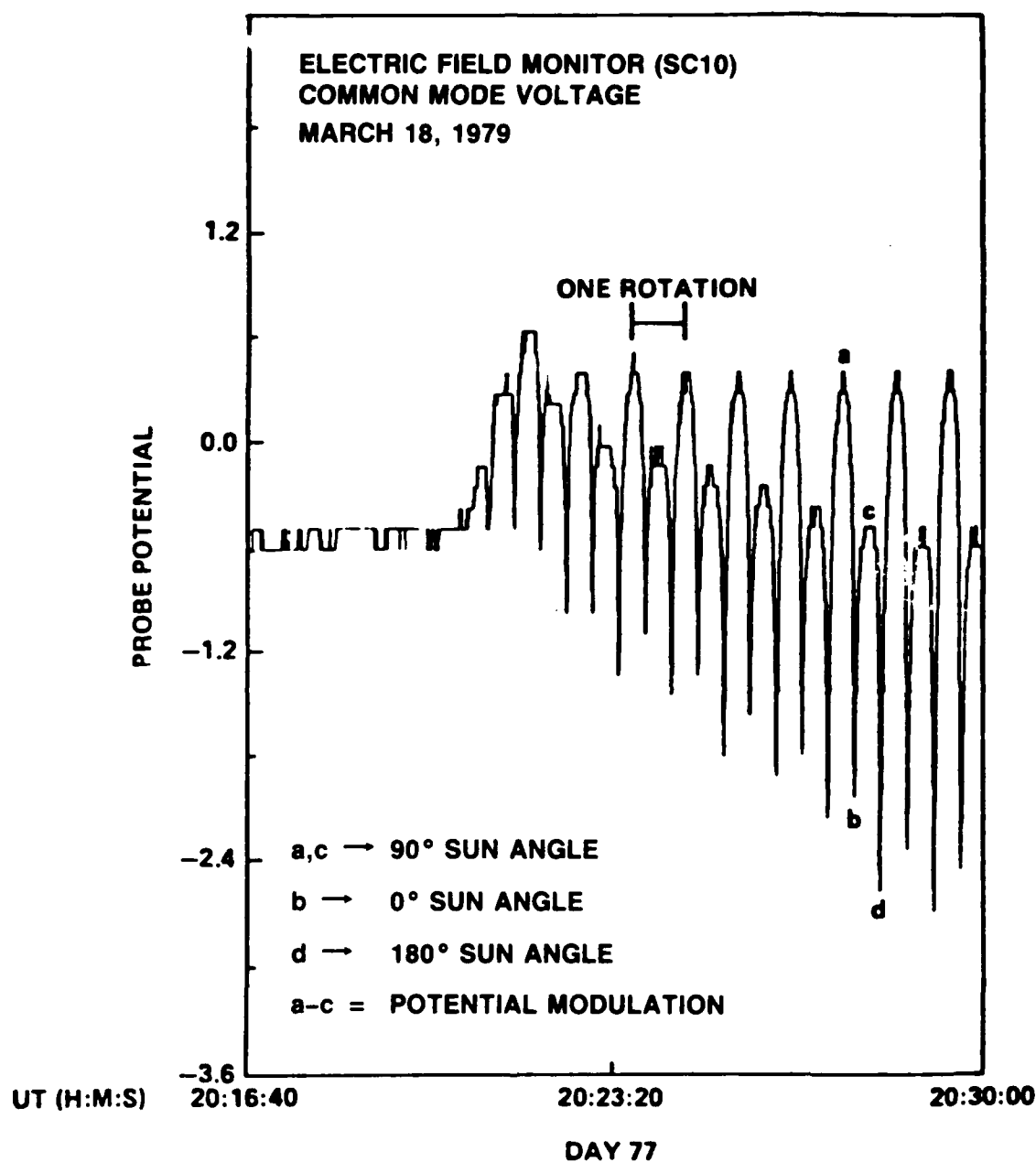


Figure 5a. Eclipse Behavior of the Field Detectors; the Behavior of the GSFC Electric Field Monitor

incidence illumination (0 and 180 deg sun angle). The length of these antennas and their location on the bottom edge of the satellite makes it difficult to say that at the 180 deg sun angle they are in the spacecraft shadow. However, the grazing incidence illumination for the cylindrically shaped antenna will appear to have the same effect as an actual blockage of sunlight. This can be seen in Figure 5a in the positions marked b (0 deg sun angle) and d (180 deg sun angle). Changes in the spacecraft ground will also cause the common mode voltage to vary. There are two positive peaks evident in the probe voltages in Figure 5a. Both occur when the antenna is 90 deg to the sun (denoted by a and c in the figure). The difference in the magnitude of the two peaks is due to a change in spacecraft ground rather than a difference in the illumination of the antenna (Aggson et al., 1983).

#### D. ECLIPSE

The association of these effects with sunlight can be confirmed by examining the behavior of the field detectors in eclipse. The pattern of the voltages for the sheath monitor and the electric field probe is shown in Figures 5a and 5b for exit from an eclipse. Figure 5b plots the potential of the SC2-1 probe and is similar to the plot in Figure 4 except that the horizontal axis is more compressed. The transition from the eclipse appears to be abrupt, as seen in Figure 5b, at about 20:21 UT. However, it takes about 5-6 spin periods before the pattern of the probe potential variation is completely re-established. This is about the time it takes for the solar array current (not shown) to reach a stable value and is indicative of a penumbral effect. However, the assymetry in the probe potential in the first two spin periods indicates that a spacecraft potential modulation is present at this time and is clearly established by the third spin period. The potential for SC10-2 is shown in Figure 5a for the same exit from eclipse as that for SC2-1 in Figure 5b. The difference in the SC10 probe voltages at perpendicular sun angles slowly increases as the satellite exits eclipse. The reappearance (disappearance) of this pattern of the data for both SC2 and SC10 as the satellite exits (enters) eclipse shows that the modulation in potential for these two probes is related to sun illumination of a part or parts of the spacecraft. The time needed to establish the pattern on exit from the eclipse

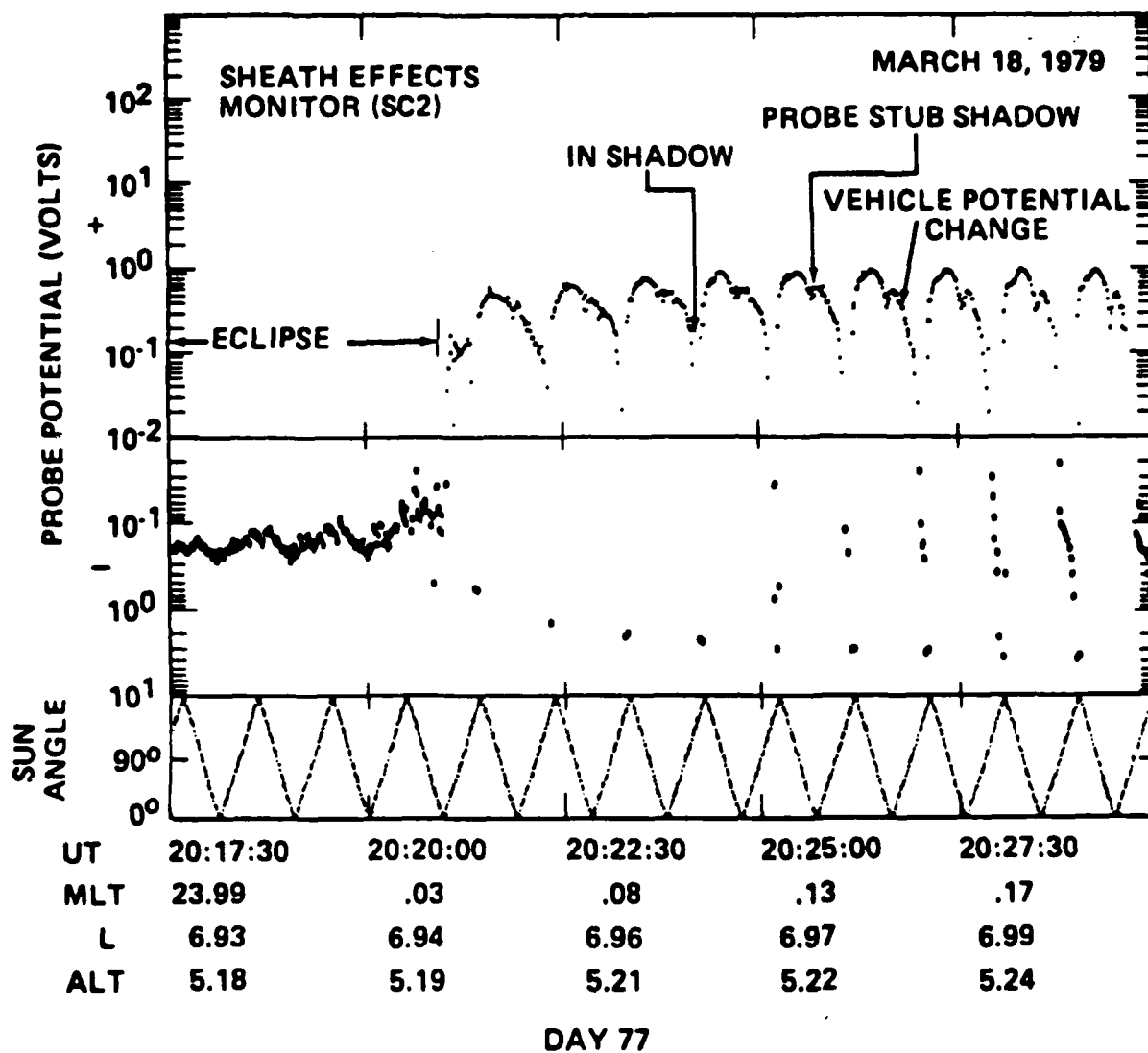


Figure 5b. Eclipse Behavior of the Field Detectors; the Behavior of the Short Booms of the Aerospace Sheath Monitor

is due in part to penumbral effects. It is also due to the time needed to establish a stable periodic potential variation as the spacecraft charges and discharges with some capacitive time constant along with all the isolated surfaces on the satellite.

The spin modulation of the potential of the electric field antenna provides a piece of information which could be quite useful for experimenters on future satellites. When the antenna is pointed towards the sun, it is effectively in eclipse; hence the drop in potential as seen, for example, in Figure 5a. The difference between the eclipse and sunlit antenna potential provides a measure of the floating potential of the satellite mainframe in sunlight. On March 18, 1979 (day 77), the antenna potential shows a spin modulation of 2 or 3 V (from +0 or +1 V to -2 V with respect to the mainframe). On this day as the satellite enters eclipse, the antenna potential attains a constant value of near 0 V with respect to the satellite. This means that in eclipse, the antenna potential and satellite potential are the same. If the antenna potential while end on to the sun is indeed the eclipse potential of the antenna, then the modulation in the antenna potential provides a measure of the difference in sunlight and eclipse satellite potentials. Since the floating potential of the satellite in eclipse is not zero, the antenna potential only provides a relative measurement. This can still be a useful element in the analysis of satellite data. In addition, other instruments on future satellites could make use of such data. In particular, aperture bias techniques, such as those used on the Dynamics Explorer 1 Retarding Ion Mass Spectrometer, would benefit from this type of feedback (Olsen et al., 1985).

#### E. PHOTOSHEATH

It is possible that the responses of the detectors are a result of an asymmetric photoelectron sheath from the spacecraft. The effects of such a sheath would most easily be seen in the responses of the field detectors. An asymmetric sheath should not affect the LIMS sensors that are on the ends of the satellite. The field detectors may be affected by a photosheath. We will use the common mode voltage measurements of these two field instruments to

show that the sheath effect on the common mode measurements is small, at least when the ambient plasma has a significant cold ion population. March 18, 1979 (day 77), provides a good example. Probes for these two instruments (remember that each instrument has two probes, 180 deg apart) reach a higher potential in one half of the spin period than in the other half (see Figures 5a and 5b) although the same sun angles are experienced in both spin halves. This behavior indicates that the responses of the antennas are caused by the modulation of the spacecraft ground. Since the sheath monitor should be within the spacecraft sheath and the electric field monitor outside it or on the edge (Aggson, 1983), the small difference in the shapes of the curves at sun angles other than 0 or 180 deg of each of the antennas shows that the sheath effect on the antenna response is small in comparison to the change in the spacecraft ground.

#### F. SUMMARY OF OBSERVATIONS

In order to pinpoint which part or parts of the spacecraft when illuminated are causing the spacecraft potential to be modulated, we plotted the modulation cycle for each of the instruments as a function of the angle between the spacecraft +Z axis and the spacecraft-sun line. This plot is shown in Figure 6. The angle between the spacecraft +Z axis and the sun is plotted along the horizontal axis. The figure axis does not start at zero in order to clearly show the two parts of the modulation cycle. The probe voltage on the vertical axis for the two field detectors is a linear scale while the particle detector axis is a log scale, reflecting the expected effect of a potential on the two types of detectors. From this figure, it is evident that all four instruments are responding to the effects of a change in spacecraft potential at the same time. The cycle is such that the potential is at a minimum when the angle between the sun and the +Z axis is between about 260 and 20 deg. A radial vector from the satellite to the sun in the center of this minimum passes very near the SC9 position.

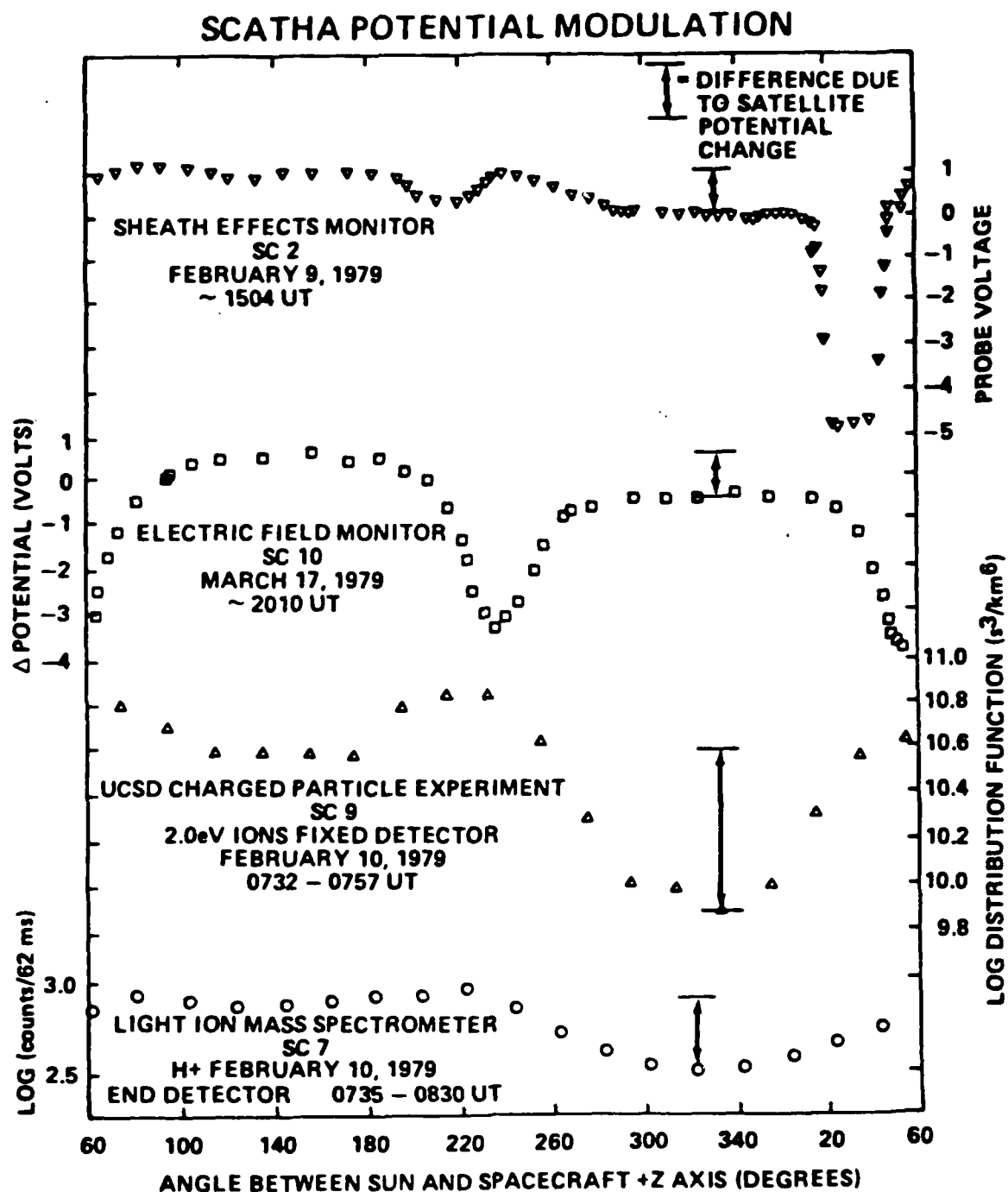


Figure 6. Modulation Cycle of All the Instruments Plotted in the Spin Phase Angle of the LIMS. At 0 deg, the SC10 antenna is 180 deg to the sun and in the satellite shadow.



### III. ANALYSIS

It is expected that the sun's illumination is a dominant factor in determining the spacecraft potential since at the geosynchronous orbit the photocurrent is the major current from the spacecraft (Knott, 1972; Grand et al., 1983). Changes in the plasma environment were not observed by either of the particle instruments during the events on February 9 and 10, 1979, so that it is not likely that the spacecraft is responding to a change in plasma characteristics. Therefore the change must be related entirely to sun illumination or more exactly to photoemission. Surface material properties are therefore suspect and in particular those materials that are likely to influence the spacecraft ground potential. Since conducting surfaces are tied to the spacecraft frame, a close examination of them is in order. Since the normal to the ends of the satellite is kept perpendicular to the sun within  $\pm 5$  deg, the materials on the forward and aft ends will not contribute significantly to the spacecraft charge, at least not through photoemission. The surface of the cylinder is mostly covered with insulating materials (e.g., solar cells). The distribution of the conducting material on the cylinder surface is shown in Figure 7. The angles in this figure increase in the direction of satellite rotation. This is opposite to the direction of the angles shown in Figure 1. Most of the conducting material is contained in the band around the middle of the cylinder that contains the instruments; however, there is a significant area of indium oxide (a conductor) on the solar cells under the SC9 instrument.

In addition to knowing the position and area of conducting material, one must also know the photoemissive properties of the materials. We used the same photoemissive values for the materials as used by Stannard et al. (1980) in an analysis of SCATHA charging. The model of the photoemissive yields for normal incidence used in this study are shown in Figure 8. Most of the surface materials have a photoelectron yield of  $2 \times 10^{-5}$  A/m<sup>2</sup> for normally incident sunlight. The photoemissive yield of the bellyband of  $2.45 \times 10^{-5}$  A/m<sup>2</sup> is the average yield of alternating stripes of gold and yellow conducting paint.

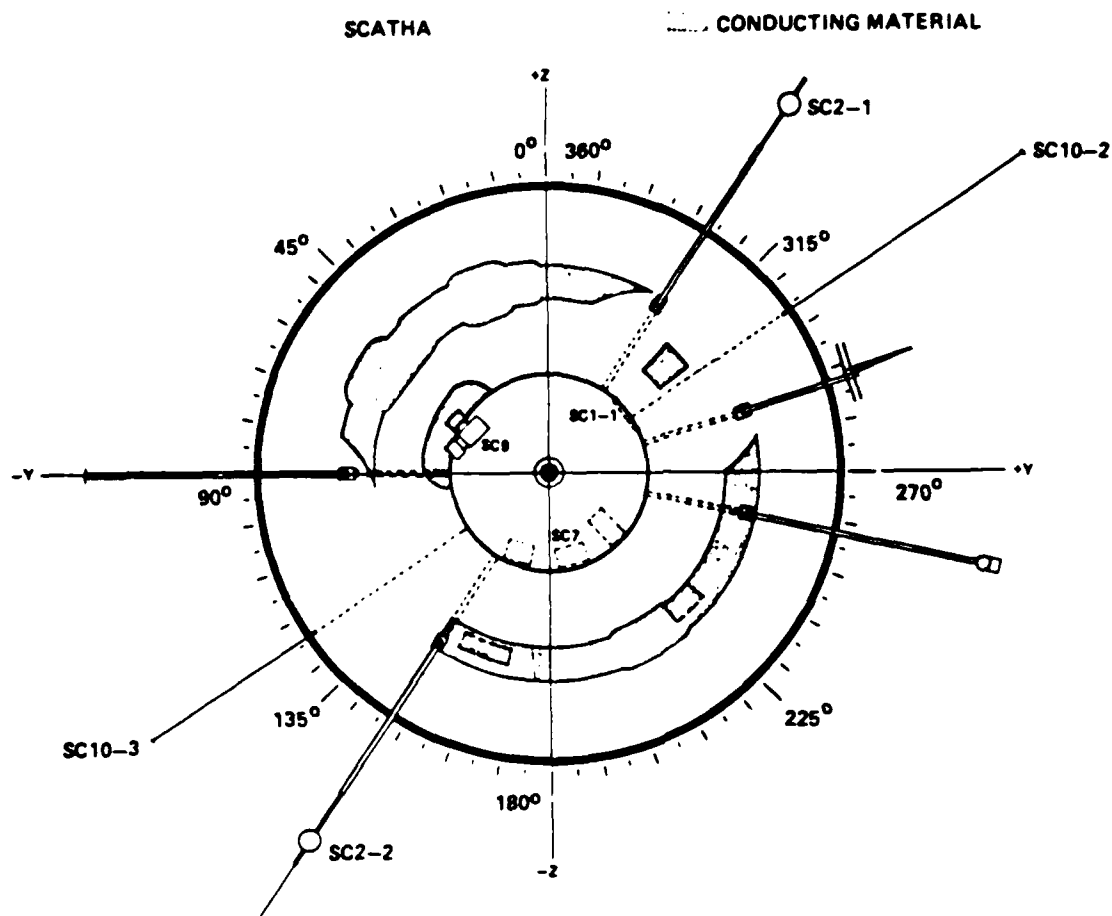


Figure 7. Distribution of Grounded Conducting Exterior Surfaces on SCATHA. The angles follow the direction of satellite rotation.

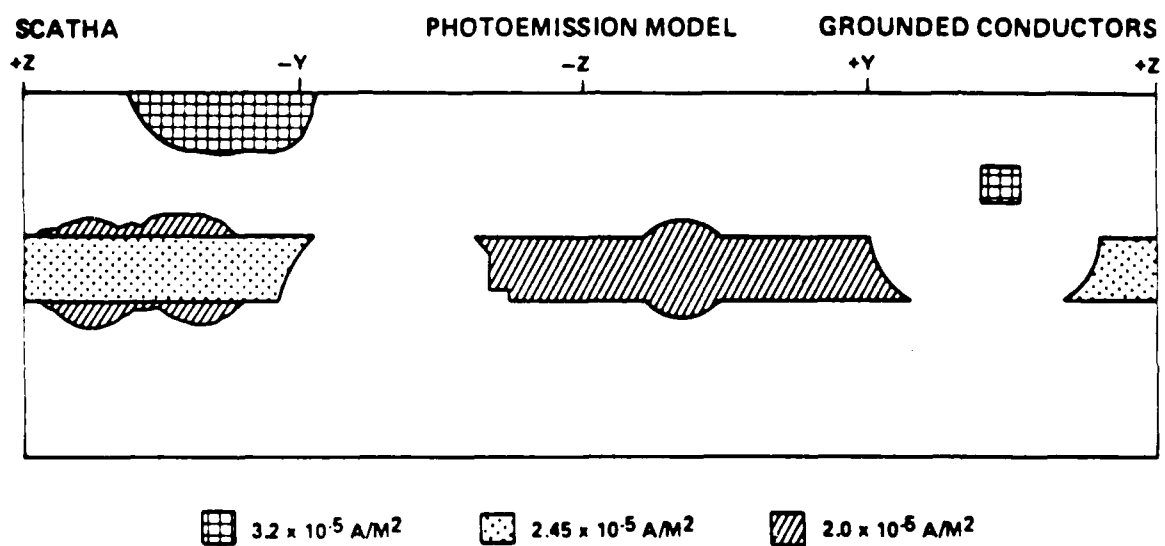


Figure 8. Plot of the Photoemissive Yield Model of SCATHA Used To Calculate the Total Photocurrent

In order to show the connection between the photoemission and the change in the spacecraft potential, we plotted the total photocurrent from the grounded conducting materials on the satellite as a function of the rotation angle from the spacecraft +Z axis. For this purpose, the cylindrical surface was divided into 10 deg bands, and the photocurrent from the different conducting materials in each 10 deg band was summed. The total photocurrent resulting from a particular orientation of the satellite was calculated by integrating the photocurrents from each band weighted by the cosine of the angle from the band to the sun. This assumes no change in the photoemissive yield, except for the decrease in area, when light is nonnormally incident. When a particular band faced the sun directly, the photocurrent from it contributed to the integral with a reduction, while those bands on either side and 90 deg or greater from the center band, i.e., 90 deg from the sun, contributed nothing to the integral.

This total photocurrent from the illuminated grounded conducting material is plotted as a function of the spacecraft rotation angle in Figure 9. The total photocurrent is plotted on the left hand scale. The counts from the LIMS sensor 2, averaged over about 60 spins, are also shown. The LIMS counts are plotted on the right hand scale. A distinct asymmetry in the photocurrent is shown. The photoemissive current from the satellite is greatest near the center of the indium oxide coating near the UCSD instrument. The large peak in calculated photocurrent seen at this point is the result of a combination of increasing conducting area and of an increase in the photoemissive yield. A smaller peak in the photocurrent is evident at about 140 deg that also coincides with the decrease in the LIMS counts from sensor 2. There is good agreement between the change in the photoemissive current and the potential cycle exhibited by the four instruments and represented by the LIMS data. It does not appear that the potential modulation is caused by an angular anisotropy of the electrons or ions (Fennell, 1981). The evidence for this comes from the fact that neither the ions nor the electrons come predominately from one direction or the other when trapped or field aligned. Since there are not two peaks per spin period in any of the instruments, the angular anisotropies in the particles are not causing the potential modulation.

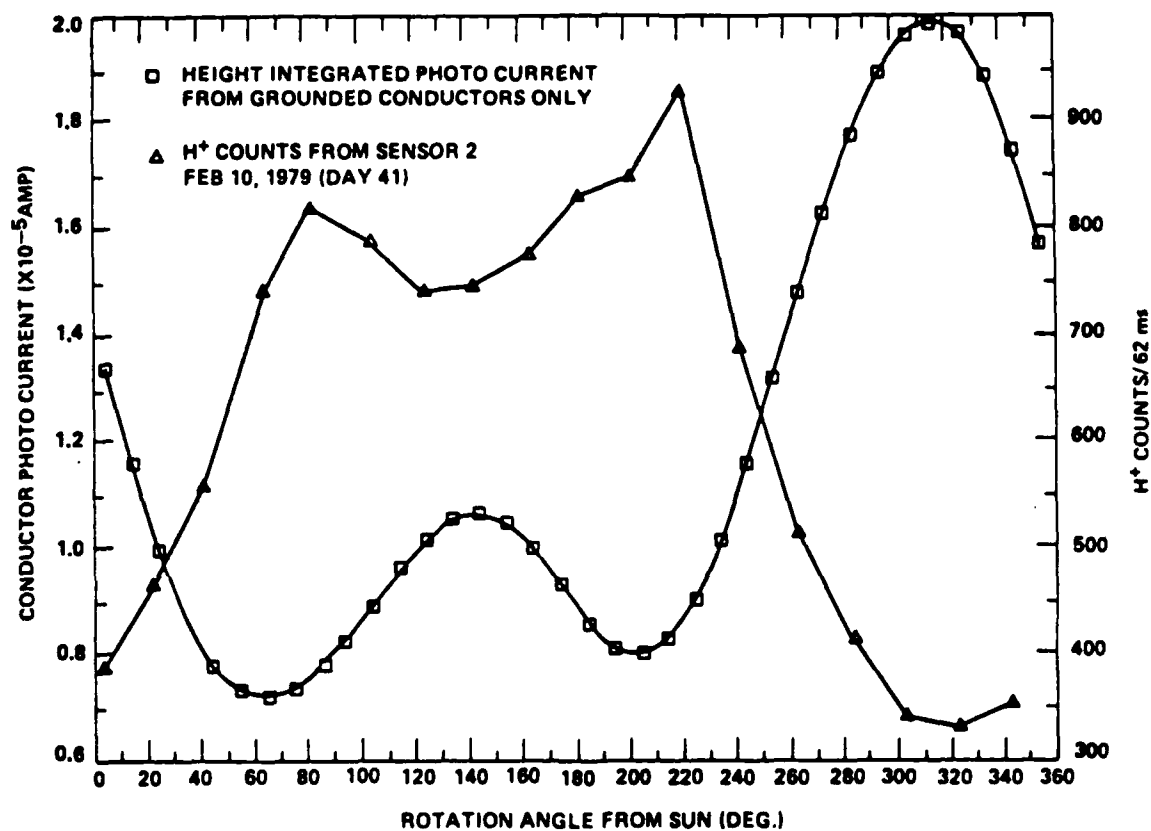


Figure 9. Total Photocurrent of Illuminated Grounded Exterior Conducting Surfaces as a Function of the +Z-Sun Angle. The +Z axis of SCATHA is at 0 deg, as shown in Figure 7.

reported on here. It thus appears that the small potential change experienced by the SCATHA satellite is due to a nonuniform distribution of the material properties of grounded conductors on the satellite. Both insulators and conductors experience photoemission, and electrons emitted by one can be collected by the other. The fact that the effects of the potential change reported on here are strongly linked to conducting materials is a result of the practice of grounding conductors directly to the spacecraft frame.

#### IV. CONCLUSIONS

We have shown that small potential changes can be experienced during the spin period of a spacecraft. The potential modulation observed on SCATHA is dominated by a nonuniform distribution of photoemissive properties of the exposed conducting materials that are directly grounded to the spacecraft frame. It does not appear that the phenomenon reported on here is a result of differential charging and a corresponding charging of the spacecraft as reported for ATS 6 by Olsen and Purvis (1983). The surfaces that are responsible for the potential change on SCATHA are grounded to the spacecraft frame and should not differentially charge. Further evidence that the effect is not due to differential charging is seen in the response of the two types of instruments. The field instruments see the effect as a change in the spacecraft ground. The particle instruments see the modulation as a result of a change in the potential of the surface near the detectors. Since all the instruments respond to the change in the same way and at the same time, it appears that the spacecraft ground and the potential of the grounded conductors are changing at the same time and in the same way.

The modulation is easily seen when the potential of the spacecraft is apparently small, i.e., on the order of several volts. On all the days examined, a cold ion population is measured in significant amounts during the time the modulation is most obvious. The density and temperature of the ion population measured by both the LIMS and the UCSD instrument on February 9 and 10 and by the UCSD instrument on March 18 (day 77) indicate that the satellite is in the outer plasmasphere during the times that the modulation is most obvious. Since the cause of the modulation is ultimately the sun's illumination, it must surely be present at other times (excluding eclipse) when the satellite is outside the plasmopause. At these times, the spacecraft potential is probably higher and the plasma population higher in temperature. In this case the potential modulation would not be so obvious in the particle data since a 1 volt higher potential would not reduce the flux into the instrument as much.

The avoidance of small potential modulations such as reported here is particularly important for low energy particle measurements. Thus, when such measurements are to be made on a spinning spacecraft that is to have passive electrostatic control, an attempt should be made to balance the material properties related to photo-electron emission. However, since it seems unlikely that material properties will be known well enough to completely avoid small potential modulations through passive control, other methods should be considered. One such method is active control of the spacecraft potential using plasma emitters (Olsen, 1981).



## REFERENCES

- Aggson, T. L., B. D. Ledlew, A. Egeland, and I. Katz, Probe Measurements of DC Electric Fields, in Proceedings of the 17th ESLAB symposium on "Spacecraft/Plasma Interactions and their Influence on Field and Particle Measurements," Noordwijk, The Netherlands, 13-16 September 1983, ES SP-198, pp. 13-17, 1983.
- Deforest, S. E., and C. E. McIlwain, Plasma Clouds in the Magnetosphere, J. Geophys. Res., 76, 3587-3611, 1971.
- DeForest, S. E., Electrostatic Potentials developed by ATS-5, in Photon and Particle Interactions with Surfaces in Space, edited by R. J. L. Grard, pp. 263-276, D. Reidel, Dordrecht, The Netherlands, 1973.
- Fennell, J. F., D. R. Croley, Jr., P. F. Mizera and J. D. Richardson, Electron Angular Distributions during Charging Events, in "Spacecraft Charging Technology 1980," NASA Conference Publication 2182 (AFGL-TR-81-0270), pp. 370-385, 1981.
- Fennell, J. F., Description of the P78-2 (SCATHA) Satellite and Experiments, in The IMS Source Book, edited by C. T. Russell and D. J. Southwood, pp. 65-81, American Geophysical Union, Washington, D.C., 1982.
- Grard, R., K. Knott and A. Pedersen, Spacecraft Charging Effects, Space Science Reviews, 34, 289, 1983.
- Knott, K., P. M. E. Decreau, A. Korth, A. Pedersen, and G.L. Wrenn, The Potential of an Electrostatically Clean Geostationary Satellite and Its Use in Plasma Diagnostics, Planet. Space Sci., 32, 227, 1984.
- Lai, S. T., and H. A. Cohen, Boom Potential of a Rotating Satellite in Sunlight, EOS (Abstract), 65, 261, 1984.
- Mauk, B. H., and C. E. McIlwain, ATS-6 Auroral Particles Experiment, IEEE Trans. Aerosp. Electron. Syst., AES-11, 1125-1130, 1975.
- Olsen, R. C., Modification of a Spacecraft Potential by Plasma Emission, J. Spacecraft and Rockets, 18, 462-469, 1981.
- Olsen, R. C., The Hidden Ion Population in the Magnetosphere, J. Geophys. Res., 87, 3481, 1982.
- Olsen, R. C., and C. K. Purvis, Observations of Charging Dynamics, J. Geophys. Res., 88, 5657, 1983.
- Reasoner, D. L., C.R. Chappell, S. A. Fields and W.J. Lewter, Light Ion Mass Spectrometer for Space Plasma Investigations, Rev. Sci. Instrum., 53, 441, 1982.

Sojka, J. J., G. L. Wrenn and J. F. E. Johnson, Pitch Angle Properties of Magnetospheric Thermal Protons and Satellite Sheath Interference in their Observation, J. Geophys. Res., 89, 9801-9811, 1984.

Stannard, P. R., I. Katz, M. J. Mandell, J. J. Cassidy, D.E. Parks, M. Rotenberg, P. G. Steen, Analysis of the Charging of the SCATHA (P78-2) Satellite, NASA Contractor Report NASA CR-165348, Lewis Research Center, Chapter 2, 1980.

Stevens, J. R., and A. L. Vampola, Editors, Description of the Space Test Program P78-2 Spacecraft and Payloads, Tech. Rep. SAMSO TR-78-24, Space and Missile Systems Organization, Los Angeles, CA., 1978.

## LABORATORY OPERATIONS

The Aerospace Corporation functions as an "architect-engineer" for national security projects, specializing in advanced military space systems. Providing research support, the corporation's Laboratory Operations conducts experimental and theoretical investigations that focus on the application of scientific and technical advances to such systems. Vital to the success of these investigations is the technical staff's wide-ranging expertise and its ability to stay current with new developments. This expertise is enhanced by a research program aimed at dealing with the many problems associated with rapidly evolving space systems. Contributing air capabilities to the research effort are these individual laboratories:

Aerophysics Laboratory: Launch vehicle and reentry fluid mechanics, heat transfer and flight dynamics; chemical and electric propulsion, propellant chemistry, chemical dynamics, environmental chemistry, trace detection; spacecraft structural mechanics, contamination, thermal and structural control; high temperature thermomechanics, gas kinetics and radiation; cw and pulsed chemical and excimer laser development including chemical kinetics, spectroscopy, optical resonators, beam control, atmospheric propagation, laser effects and countermeasures.

Chemistry and Physics Laboratory: Atmospheric chemical reactions, atmospheric optics, light scattering, state-specific chemical reactions and radiative signatures of missile plumes, sensor out-of-field-of-view rejection, applied laser spectroscopy, laser chemistry, laser optoelectronics, solar cell physics, battery electrochemistry, space vacuum and radiation effects on materials, lubrication and surface phenomena, thermionic emission, photo-sensitive materials and detectors, atomic frequency standards, and environmental chemistry.

Computer Science Laboratory: Program verification, program translation, performance-sensitive system design, distributed architectures for spaceborne computers, fault-tolerant computer systems, artificial intelligence, microelectronics applications, communication protocols, and computer security.

Electronics Research Laboratory: Microelectronics, solid-state device physics, compound semiconductor radiation hardening; electro-optics, quantum electronics, solid-state lasers, optical propagation and communications; microwave semiconductor devices, microwave/millimeter wave measurements, diagnostics and radiometry, microwave/millimeter wave thermionic devices; atomic time and frequency standards; antennas, rf systems, electromagnetic propagation phenomena, space communication systems.

Materials Sciences Laboratory: Development of new materials: metals, alloys, ceramics, polymers and their composites, and new forms of carbon; non-destructive evaluation, component failure analysis and reliability; fracture mechanics and stress corrosion; analysis and evaluation of materials at cryogenic and elevated temperatures as well as in space and enemy-induced environments.

Space Sciences Laboratory: Magnetospheric, auroral and cosmic ray physics, wave-particle interactions, magnetospheric plasma waves; atmospheric and ionospheric physics, density and composition of the upper atmosphere, remote sensing using atmospheric radiation; solar physics, infrared astronomy, infrared signature analysis; effects of solar activity, magnetic storms and nuclear explosions on the earth's atmosphere, ionosphere and magnetosphere; effects of electromagnetic and particulate radiations on space systems; space instrumentation.

END

3-87

DTIC